J Solid State Electrochem (2011) 15:615–621
DOI 10.1007/s10008-010-1135-4

ORIGINAL PAPER

Cathodic behavior of graphite in KF-AlF_3-based melts with various cryolite ratios

Dongren Liu · Zhanhong Yang · Wangxing Li · Suqin Wang · Shenwei Wang

Received: 28 March 2010 / Revised: 22 June 2010 / Accepted: 23 June 2010 / Published online: 7 July 2010

Abstract The cathodic behavior of graphite in KF-AlF_3-based melt with various cryolite ratios (CR; molar ratio of KF to AlF_3) were investigated by means of cyclic voltammetry, sampled-current voltammetry, and chronopotentiometry. The limiting current of aluminum deposition and critical current density of potassium intercalation on graphite cathode in KF-AlF_3-based melt decreased with the increase of CR of the melt. Lowering the CR of KF-AlF_3-based melt suppressed the potassium intercalation but enhanced the formation of aluminum carbide. In the KF-AlF_3-based melt with CR of 1.0, formation of Al_4C_3 seriously occurred, which resulted not only from the chemical reaction of aluminum and carbon but also from the electrochemical reduction of carbon under higher overpotential. However, both the X-ray diffraction and scanning electron microscopy failed to detect the existence of potassium–graphite intercalation compound and Al_4C_3 in the resultants after galvanostatic electrolysis.

Keywords Graphite · KF-AlF_3-based melt · Cryolite ratio · Cathode behavior · Aluminum electrolysis

D. Liu · Z. Yang (✉) · S. Wang · S. Wang
School of Chemistry and Chemical Engineering,
Central South University,
Changsha 410083 Hunan, China
e-mail: zhyang@mail.csu.edu.cn

W. Li
Zhengzhou Research Institute of Chalco,
Zhengzhou 450041 Henan, China

D. Liu
Department of Chemical and Environmental Engineering,
Jiaozuo University,
Jiaozuo 454003 Henan, China

Introduction

Due to the advantages of low energy consumption and low heat loss, low-temperature aluminum electrolysis contributes to energy saving. Also, low-temperature electrolysis can facilitate the application of inert anode to the Hall–Héroult process because the erosion rate of the inert anode would be greatly reduced at low temperature [1–3]. Compared with LiF-AlF_3-based and NaF-AlF_3-based systems, KF-AlF_3-based system is considered as a potential low-temperature electrolyte for aluminum electrolysis owing to its lower eutectic temperature and higher alumina solubility [4–6]. However, the stronger penetrations of KF-AlF_3-based melt and potassium into carbon cathode at higher temperature, which would greatly shorten the life of aluminum reduction cell, hindered its industrial application. The KF-AlF_3-based system has attracted increasing interests in recent years [5–8], which was mainly focused on its physical or chemical properties and the corrosion on various inert anodes. However, the interaction between this system and carbon cathode is not yet fully understood. Despite the potential use of titanium diboride as "inert" cathode material [9–11], either in pure form or as composites, understanding of the interaction between KF-AlF_3-based melt and carbon is still important to predict the performance of carbon cathode when KF-AlF_3-based melt is used as electrolyte for aluminum electrolysis.

Several kinds of alkaline metals (such as K, Na, and Li) can intercalate into graphite in various molten salts [12–15]. Intercalation of alkaline metal into graphite in molten salt, especially the intercalant with larger ion radius, would lead to lattice expansion and even the total destruction of graphite. A typical example is the intercalation of sodium into carbon cathode in cryolite melt during aluminum electrolysis, which is the main reason for the cathode swelling [16–19]. Similarly, the reaction between potassium and carbon cathode is believed

to play a major role during the cathode degradation process when KF-AlF_3-based melt is used as electrolyte. The intercalation of potassium into graphite in KF melt has been reported [20] and the electrochemical behavior of graphite in KF-AlF_3-based melt with a cryolite ratio (CR) of 1.3 at 750 °C has been studied [21]. In KF melt, potassium intercalated into graphite cathode and a dilute potassium–graphite intercalation compound (K-GIC) was formed during cathodic polarization. In KF-AlF_3-based melt, the intercalation of potassium occurred at a potential which is about 0.35 V more negative than that of aluminum deposition. Because the concentration of aluminum-containing complex ions vary with the molar ratio of KF to AlF_3 in the melt, the CR of KF-AlF_3-based system must have some effects on the aluminum deposition and potassium intercalation. In the present work, the cathodic behavior of graphite in KF-AlF_3-based melts with various CR was discussed, with the aim of understanding the role of CR in the cathodic polarization process.

Experimental

Preparation of the electrolyte

The preparation of KF-AlF_3-based electrolyte with a CR of 1.3 was introduced in our earlier work [21]. Similar to that, KF-AlF_3-based electrolytes with the CR of 1.0 (containing 40.89 wt.% KF and 59.11 wt.% AlF_3), 1.5 (containing 50.93 wt.% KF and 49.07 wt.% AlF_3), and 1.8 (containing 55.46 wt.% KF and 44.54 wt.% AlF_3) were also prepared from individual KF and AlF_3 salts. Before use, anhydrous KF was dried at 250 °C under vacuum for 12 h and then stored in a glove box filled with high purity nitrogen. AlF_3 was pretreated by heating with NH_4HF_2 at 200 °C for 5 h and then at 500 °C for 6 h to get rid of most of the Al_2O_3 impurity. After pretreatment, the KF and AlF_3 with various molar ratios were homogeneously mixed in the glove box by continuous grinding with a muller. The mixture with a total mass of 250 g was then transferred to a graphite crucible container. The crucible was heated in the flow of nitrogen by elevating temperature to 600 °C for 3 h and then to the working temperature of 850 °C. The melt was held at 850 °C for 2 h before performing electrochemical measurements. By using a LECO TC-136 Oxygen/Nitrogen Determinator, which was equipped with a halogen absorber to capture the fluoride vapor and thereby to prevent the detector from damage [4, 5], all the oxygen contents in the prepared electrolytes were determined to be <0.2 wt.%. All reagents used were analytical grade.

Experimental apparatus

Electrochemical experiments were performed with a three-terminal electrochemical cell. The graphite crucible served as container for the melt and also as the high surface counter electrode. The working electrode (WE) was a spectral pure graphite rod with a diameter of 6 mm, which was mechanically inserted into a pyrolytic boron nitride (BN) tube with an inner diameter of 6 mm until the cross section of the graphite rod and the end of the BN tube were in the same level. The cross section of the graphite rod was polished with increasingly finer grades of emery paper. Stainless steel rod was connected to the WE as current lead. After assembly, the WE was immersed into the melt and the cross section of the graphite rod was exposed to the melt. The working area of the WE was 0.283 cm^2. Liquid aluminum contained in a corundum tube was employed as reference electrode (RE). The corundum tube was entirely shielded with thin sintered BN tube to prevent it from dissolution. During the experiments, the electrolyte penetrated the sintered BN tube and contacted with the liquid aluminum through a 0.5-mm hole in the side wall of the corundum tube. A tungsten wire shielded with corundum tube was inserted into the liquid aluminum and served as current leader. All potentials in the present work were expressed with respect to the aluminum RE. The RE was dipped into the melt and stood at least 2 h until a stable electrode potential was established before electrochemical measurements. The stability of the aluminum RE was evaluated by measuring the potential difference between a platinum wire and the RE immersed in the fluoride melt for 12 h. It was found that the potential fluctuation of RE did not exceed ±20 mV. The graphite crucible was placed inside a sintered corundum tube within a programmable vertical furnace. The electrochemical cell was under a continuous nitrogen flow during the experiment.

Electrochemical measurements

The WE was characterized by means of cyclic voltammetry, sampled-current voltammetry, and chronopotentiometry. Around 80% of the measured melt resistance between the WE and RE was compensated for all cyclic voltammetry and sampled-current voltammetry measurements. After every potential step and current step experiment, the WE was oxidized by using 30 mA anodic current until the carbon dioxide was emitted and the melt was purged for 5 min. Electrochemical measurements were performed with a PAR Model 263A Potentiostat/Galvanostat.

Results and discussion

Cyclic voltammetry

Figure 1 presents the cyclic voltammogram recorded on graphite in KF-AlF_3-based melt (CR=1.3) at a sweep rate of 100 mV s^{-1} and a temperature of 850 °C, which is very similar to that of graphite in this melt at 750 °C [21]. It has

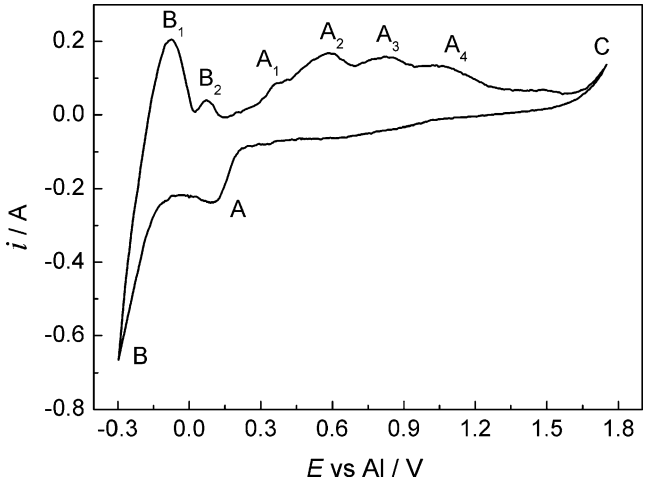

Fig. 1 Cyclic voltammogram recorded on graphite electrode in KF-AlF_3-based melt (CR=1.3) at a scan rate of 100 mV s^{-1} and a temperature of 850 °C

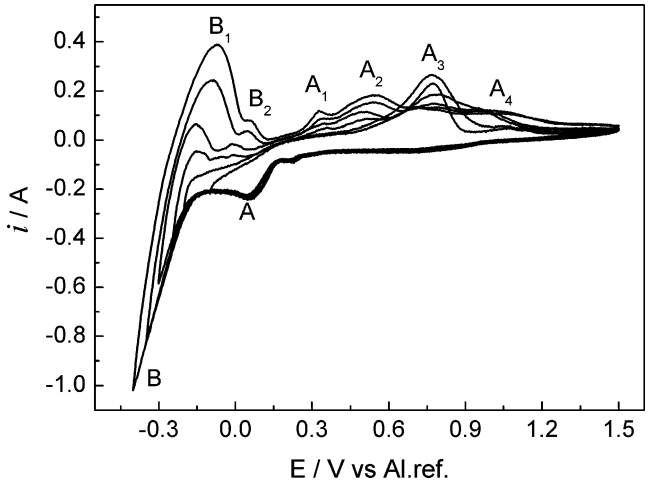

Fig. 2 Cyclic voltammograms recorded on graphite electrode with various cathodic limits in KF-AlF_3-based melt (CR=1.3) at a scan rate of 100 mV s^{-1} and a temperature of 850 °C

been demonstrated that the cathodic wave A with the onset of approximately 0.25 V is associated with the deposition of aluminum and the cathodic wave B started at approximately −0.15 V corresponds to the potassium intercalation. In the reverse sweep, the waves B_1 and B_2 are associated with the deintercalation of potassium and the stripping of the Al–K alloy, respectively. The waves A_1 and A_2 correspond to the oxidation of carbon from aluminum carbide dissolved in the melt and absorbed on the graphite surface, respectively. The wave A_3 results from the stripping of liquid aluminum. The wave A_4, which corresponds to the extraction of aluminum bonded with carbon, indicates that surface chemical reaction between aluminum and graphite seriously occurs when potassium intercalation takes place and high cathodic overpotential is applied. As an oxygen-containing melt, the wave C that started at approximately 1.7 V corresponds to the evolution of carbon dioxide.

Figure 2 depicts the cyclic voltammograms of graphite in KF-AlF_3-based melt (CR=1.3) with various cathodic switch potentials. An inspection of those voltammograms shows that only wave A_3 appears at the anodic sweep when the sweep reverses at the potential more positive than −0.15 V, indicating that the thermodynamically favored formation of Al_4C_3 is quite mild when lower overpotential is applied. This is probably due to the fact that the reaction rate of aluminum and carbon is slow, while a relatively fast potential sweep is applied. However, waves A_1, A_2, and A_4 start to emerge when the cathodic switch potential is more negative than −0.15 V. Furthermore, at the expense of reducing the peak current of wave A_3, the peak currents of waves B_1, A_1, A_2, and A_4 increase and the width of wave A_3 broadens as the cathodic switch potential becomes more negative than −0.15 V. These behaviors suggest that the formation of aluminum carbide is accelerated by the intercalation of potassium and the higher cathodic overpotential. As revealed in reference [20], the intercalation of potassium greatly erodes graphite and destroys its structure. Apparently, the potassium intercalation and the formation of aluminum carbide, as the side reactions of aluminum production, reduce the current efficiency of aluminum electrolysis. From the analyses above, it is predictable that, in the industrial aluminum reduction cell, the higher cathodic overpotential would accelerate the degradation of carbon cathode and greatly lower the current efficiency when KF-AlF_3-based melt is used as electrolyte.

The cyclic voltammetric behaviors of graphite in the KF-AlF_3-based melts with various CR are presented in Fig. 3. The peak current and peak area of the cathodic wave

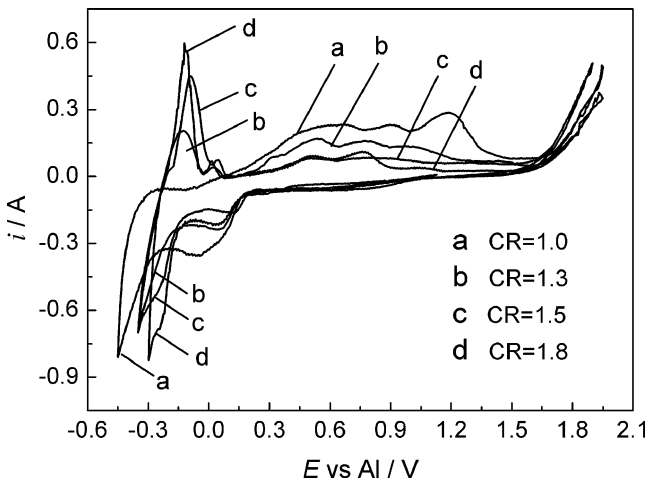

Fig. 3 Cyclic voltammograms recorded on graphite electrode in KF-AlF_3-based melt with various CR at a scan rate of 100 mV s^{-1} and a temperature of 850 °C

associated with aluminum deposition decrease with the increase of CR. This is probably due to the fact that the concentration of reducible anion (AlF_4^-) in the melt decreases as the CR increases. However, as CR decreases, the peak current and area of cathodic wave of potassium intercalation are depressed, indicating that potassium intercalation is facilitated in the melt with higher CR. At the positive sweep, the wave of aluminum carbide oxidation is apparently strengthened as the CR decreases, suggesting that the formation of Al_4C_3 becomes more serious in lower CR melt than in higher CR melt. The cyclic voltammograms of graphite in melt with CR of 1.3, 1.5, and 1.8 display similar features; however, the cyclic voltammetric behavior of graphite in the KF-AlF_3-based melts with CR of 1.0 is quite different from others. The voltammograms of graphite in this melt with various cathodic limits are presented in Fig. 4. Two cathodic waves, A and B, are still in existence in the cathodic sweep. However, the onset potential (approximately −0.2 V) of cathodic wave B is more negative than those in melts with higher CR. Also, the anodic waves of potassium deintercalation and Al–K alloy stripping at the reverse sweep are almost absent. These phenomena indicate that the potassium intercalation is blocked in this melt. It is also discernible that the two waves of carbon oxidation from dissolved and absorbed aluminum carbide are merged and the extraction wave of aluminum from aluminum carbide is much stronger than those in melts with higher CR. Furthermore, the anodic wave of aluminum stripping (wave A_2) shows a very wide form even when the negative sweep is switched at potentials more positive than −0.15 V. These behaviors mentioned above indicate that the formation of Al_4C_3 seriously occurs in the melt with CR of 1.0 even when no potassium intercalation occurs. Although aluminum carbide can dissolve in the acidic fluoride melt [22, 23], the Al_4C_3 formed on the graphite surface during the cathodic sweep cannot completely dissolve because a relatively fast sweep rate is applied. Consequently, the undissolved Al_4C_3 film covers the graphite surface and subsequently prevents the graphite from potassium insertion. As demonstrated in a previous paper [21], the formation of Al–K alloy started at approximately −0.35 V (vs. Al) and the metallic potassium deposited at approximately −0.6 V(vs. Al) at 750 °C. Because the wave B in Fig. 4 starts at approximately −0.2 V, the metallic potassium deposition and formation of Al–K alloys would not occur. Considering the absence of potassium deintercalation in the reverse sweep, the wave B in Fig. 4 is supposed to be not associated with the potassium intercalation but with the electrochemical formation of aluminum carbide, i.e.:

$$4AlF_4^- + 3C + 12e = Al_4C_3 + 16F^-. \quad (1)$$

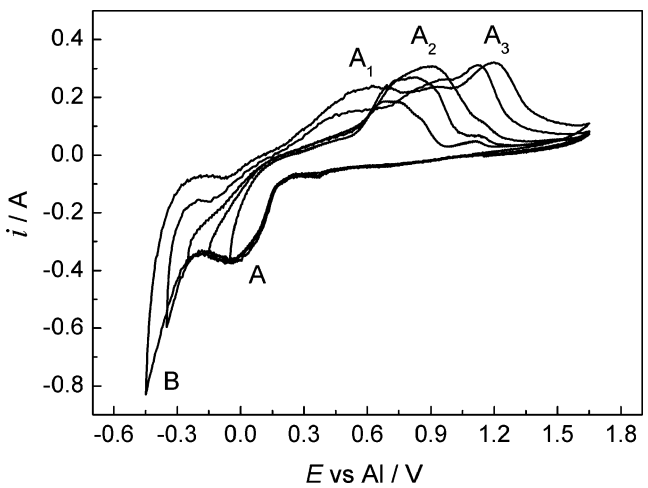

Fig. 4 Cyclic voltammograms recorded on graphite electrode with various cathodic limits in KF-AlF_3-based melt (CR=1.0) at a scan rate of 100 mV s^{-1} and a temperature of 850 °C

Sampled-current voltammetry

Sampled-current voltammograms of graphite in KF-AlF_3-based melt with various CR are shown in Fig. 5. These transients were obtained by stepping the electrode potential from an initial value to the potential of interest. The current was sampled at 10 s following the application of each step. The voltammogram of graphite in melt with CR of 1.3 at 850 °C, which is very similar to that at 750 °C, displays an ill-defined limiting current in the potential range extending from approximately 0.05 to −0.2 V. The limiting current results from the mass-transport-limited deposition of aluminum. The ill-defined limiting current probably results from the adsorption of AlF_2^+ as well as neutral species (AlF_3) on the surface of graphite cathode. As a result of adsorption, the active area of the electrode was partially blocked by the adsorbates. At more negative potential, the absorbed species are reduced and then the active area of the electrode is restored. The formation of a partly insulating layer of aluminum carbide on the graphite surface also contributes to the obstruction of the active area of the electrode. The voltammogram of graphite in the melt with CR of 1.8 also shows a limiting current plateau with a magnitude lower than that in the melt with CR of 1.3. The lower current plateau is probably due to the fact that the concentration of reducible anion (AlF_4^-) in the melt with CR of 1.8 is lower than that in the melt with CR of 1.3. However, no limiting current plateau is observed in the voltammogram of graphite in the melt with CR of 1.0. As revealed by cyclic voltammetry results, formation of Al_4C_3 seriously occurs in the melt with CR of 1.0 when aluminum deposits. As a result, the undissolved Al_4C_3 absorbs on the graphite surface and thereafter prevents the passage of electricity. Moreover, the active surface of graphite cannot be restored because the absorbed Al_4C_3 is unreducible at

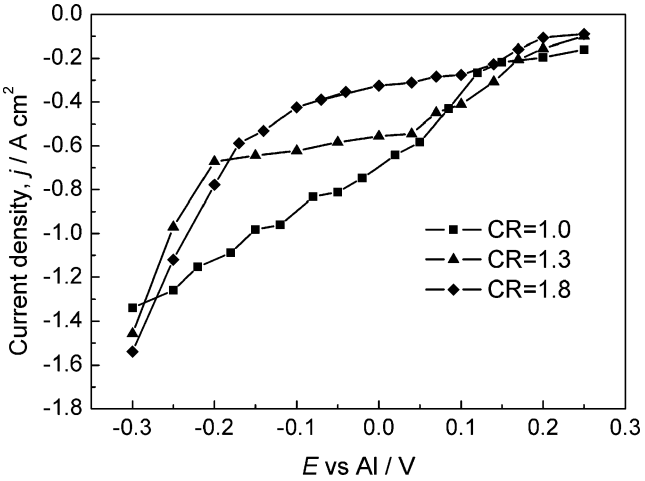

Fig. 5 Sampled-current voltammograms of graphite electrode constructed from a series of current–time transients in KF-AlF_3-based melt with various CR at 850 °C

more negative potentials. As the potential becomes negative, the active area decreases because Al_4C_3 formation continues to proceed. The higher cathodic overpotential cannot result in the mass-transfer-limited case because of the higher AlF_4^- concentration and small active area. Consequently, no limiting current on the graphite electrode appears in this melt. In the negative potential side of the limiting current plateau, the voltammograms of graphite in melt with CR of 1.3 and 1.8 display rapid current increases, which are due to the potassium intercalation into graphite.

Chronopotentiometry

Typical chronopotentiograms obtained on graphite electrode in KF-AlF_3-based melt with various CR are shown in Fig. 6. According to the voltammetric results, the potassium intercalation occurs at approximately −0.15 and −0.1 V in the melt with CR of 1.3 and 1.8, respectively. Inspection of Fig. 6 shows that the potential reaches −0.15 V in the melt with CR of 1.3 when a current density of −400 mA cm^{-2} is applied. However, when a current density of −200 mA cm^{-2} is imposed on the graphite electrode in the melt with CR of 1.8, the potassium intercalation takes place as the electrode potential gets to −0.1 V. In the melt with CR of 1.0, the undissolved Al_4C_3 on the graphite surface blocks the potassium insertion into the graphite lattice. The higher cathodic overpotential just causes the electrochemical reduction of carbon. Thus, it can be concluded that, in the melt with CR of 1.3 and 1.8, the critical cathodic current density of potassium intercalation into graphite is about −400 and −200 mA cm^{-2}, respectively.

XRD characterizations

Figure 7 presents the X-ray diffraction (XRD) patterns of the resultants on graphite cathode after galvanostatic electrolysis in KF-AlF_3-Al_2O_3-based melt with various CR at 850 °C for 2 h. The XRD measurements were performed on the X'Pert Pro diffractometer (PANalytical) with CuKα radiation. The applied cathodic current density (550 mA cm^{-2}) is higher than the critical cathodic current density of potassium intercalation. The peaks at 26.5°, 42.5°, and 54.5° are the diffraction lines of graphite. The diffraction lines at 14.4°, 24.9°, 28.9°, 35.5°, 44.1°, 51.3°, 53.3°, 60.1°, and 71.8° are the diffraction reflections of $KAlF_4$. The diffraction peaks of K_3AlF_6 locate at the positions of 18.1°, 29.9°, 36.8°, and 62.1°. The diffraction lines of aluminum appear at 38.4°, 44.7°, and 65.1°. The diffraction line at 12.8° is associated with KAl_4F_{13}. Other peaks of KAl_4F_{13} are overlapped with those of $KAlF_4$. According to the chronopotentiometric results, the applied current density can result in the potassium intercalation and accelerate the Al_4C_3 formation. However, no evidence is

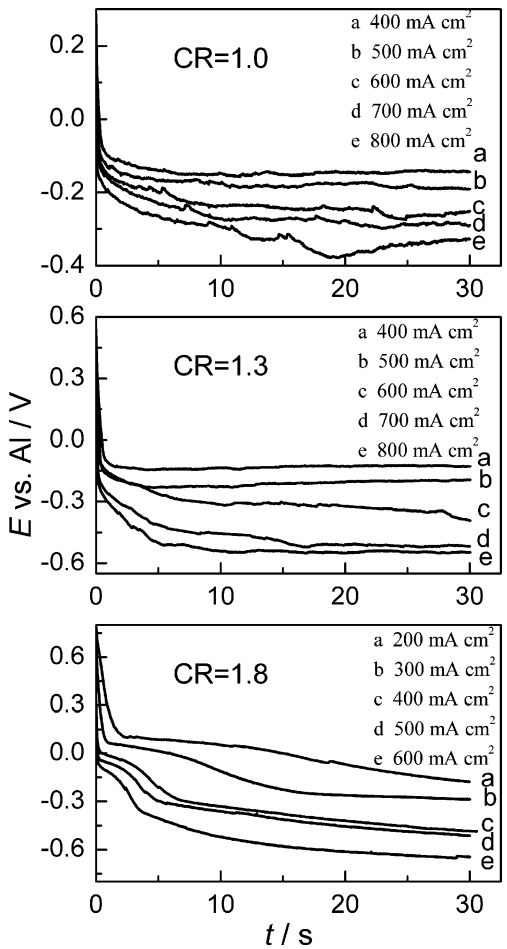

Fig. 6 Chronopotentiograms of graphite electrode in KF-AlF_3-based melt with various CR at 850 °C

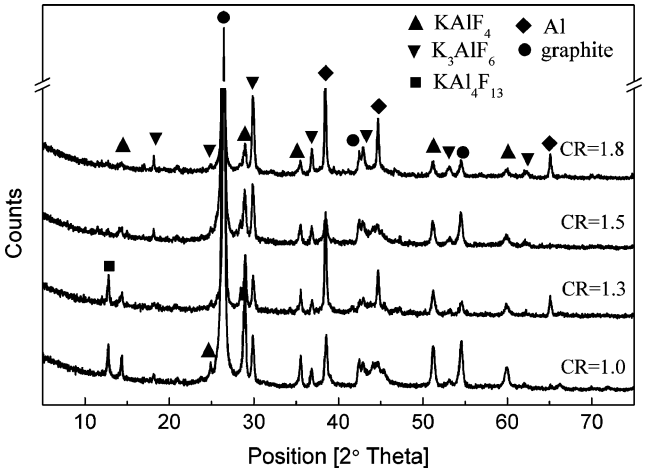

Fig. 7 XRD patterns of the resultants on graphite surface after galvanostatic electrolysis in KF-AlF_3-Al_2O_3-based melt with various CR at 850 °C

found in all the XRD patterns for the presence of K-GIC and Al_4C_3. That is probably due to the fact that K-GIC is very instable and rapidly decomposes in the high-temperature melt. As reported in the literature [18, 19, 24], aluminum carbide formed on this experimental scale is usually undetectable by using XRD measurement. Because most of the aluminum carbide would dissolve in the fluoride melt, the amount of the undissolved species is probably lower than the detection limit of the XRD.

SEM observations

Figure 8 presents the scanning electron microscopy (SEM; JSM-6360LV, JEOM) images of the longitudinal section of graphite electrode after galvanostatic electrolysis for 2 h at a cathodic current density of 550 mA cm^{-2} in KF-AlF_3-Al_2O_3-based melt with various CR at 850 °C. In those images, the dark part represents the graphite and the bright part stands for the aluminum or the solidified electrolyte.

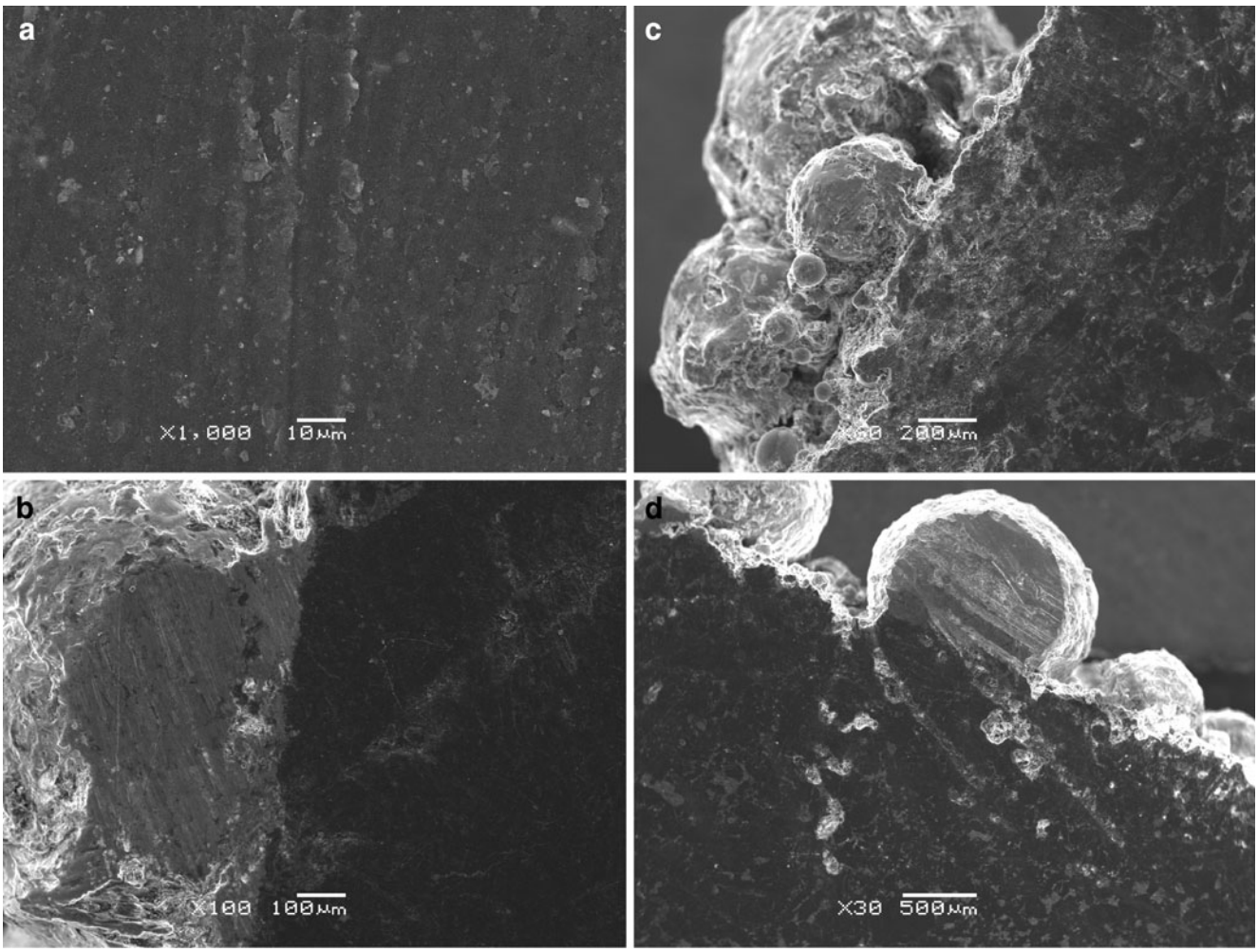

Fig. 8 **a** SEM image of the graphite electrode surface before electrolysis; **b–d** SEM images of the longitudinal section of graphite electrode after electrolysis in KF-AlF_3-Al_2O_3-based melt with CR of 1.3, 1.5, and 1.8, respectively

Before electrolysis (Fig. 8a), the graphite owns a scale-like surface. After electrolysis in the fluoride melt with various CR (Fig. 8b–d), the interface of graphite and electrolyte or aluminum becomes quite indented, suggesting that irregular crystal facets and concaves exist on the surface of the graphite electrode. As described in previous papers [20, 21], those crystal facets and concaves are believed to result from the exfoliation of graphite layers and particles from the graphite matrix caused by potassium intercalation. The SEM observations provide clear evidences that potassium intercalation occurs when depositing at the current density of 550 mA cm^{-2} in the melt with various CR. Similar to the XRD measurements, the SEM observations also fail to detect the occurrence of aluminum carbide.

Conclusions

From this study, it is found that, during the cathodic polarization process on graphite electrode, the CR of KF-AlF_3-based melt has impacts not only on the aluminum deposition but also on the potassium intercalation and aluminum carbide formation. The limiting current of aluminum deposition is diminished in KF-AlF_3-based melt with higher CR due to the lower concentration of reducible anion (AlF_4^-) in the melt. Also, the critical current density of potassium intercalation decreases with the increase of CR of KF-AlF_3-based melt. Lowering the CR of KF-AlF_3-based melt suppresses the potassium intercalation into graphite cathode but enhances the formation of aluminum carbide. In the KF-AlF_3-based melt with CR of 1.0, the formation of Al_4C_3 results not only from the combination of aluminum and carbon at high temperature but also from the electrochemical reduction of carbon under high overpotential. However, the XRD and SEM measurements fail to detect the occurrences of K-GIC and Al_4C_3 in the resultants after galvanostatic electrolysis with a cathodic current density of −550 mA cm^{-2}. From the standpoints of cathode lifetime and current efficiency, the KF-AlF_3-based melt with CR of 1.3 is the optimal system for low-temperature aluminum electrolysis because the formation of aluminum carbide and the potassium intercalation are moderate in this system. Also, this system has a very low eutectic temperature (around 600 °C). These results are of practical relevance to aluminum production when KF-AlF_3-based melt is used as low-temperature electrolyte.

Acknowledgement This work is supported by Hunan Province Innovation Foundation for Postgraduate.

References

1. Thonstad J, Olsen E (2001) JOM 53:39–42
2. Blinov V, Polyakov P, Thonstad J, Ivanov V, Pankov E (1997) Aluminium 73:906–912
3. Blinov V, Polyakov P, Thonstad J, Ivanov V, Pankov E (1998) Aluminium 74:349–351
4. Robert E, Olsen JE, Danek V, Tixhon E, Østvold T, Gilbert B (1997) J Phys Chem B 101:9447–9457
5. Yang J, Graczyk DG, Wunsch C, Hryn JN (2007) Light Met 537–541
6. Zaikov Y, Khramov A, Kovrov V, Kryukovsky V, Apisarov A, Tkacheva O, Chemesov O, Shurov N (2008) Light Met 505–508
7. Híveš J, Thonstad J (2004) Electrochim Acta 49:5111–5114
8. Dedyukhin AE, Apisarov AP, Redkin AA, Tkacheva OY, Zaikov YP (2008) Light Met 509–511
9. Sorlie M, Øye HA (1989) Cathodes in aluminum electrolysis. Aluminum, Dusseldorf
10. Xue J, Liu Q, Ou W (2007) Light Met 1061–1066
11. Thonstad J, Fellner P, Haarberg GM, Híveš J, Kvande H, Sterten Â (2001) Aluminium electrolysis: fundamentals of the Hall–Hérout process, 3rd edn. Aluminium, Dusseldorf
12. Hsu WK, Hare JP, Terrones M, Kroto HW, Walton DRM, Harris PJF (1995) Nature 377:687
13. Hsu WK, Terrones M, Hare JP, Terrones H, Kroto HW, Walton DRM (1996) Chem Phys Lett 262:161–166
14. Xu Q, Schwandt C, Chen GZ, Fray DJ (2002) J Electroanal Chem 530:16–22
15. Dimitrov AT, Chen GZ, Kinloch IA, Fray DJ (2002) Electrochim Acta 48:91–102
16. Zolochevsky A, Hop JG, Servant G, Foosnæs T, Øye HA (2003) Carbon 41:497–505
17. Zolochevsky A, Hop JG, Servant G, Foosnæs T, Øye HA (2005) Carbon 43:1222–1230
18. Brilloit P, Lossius LP, Øye HA (1993) Metall Trans B 24B:75–89
19. Lossius LP, Øye HA (2000) Metall Trans B 31B:1213–1224
20. Liu D, Yang Z, Li W, Qiu S, Luo Y (2010) Electrochim Acta 55:1013–1018
21. Liu D, Yang Z, Li W (2010) J Electrochem Soc 157:D417–D421
22. Øldegård R, Sterten Å, Thonstad J (1987) J Electrochem Soc 134:1088–1092
23. Øldegård R, Midtlyng SH (1991) J Electrochem Soc 138:2612–2617
24. Zoukel A, Chartrand P, Soucy G (2009) Light Met 1123–1128